Environmental Technology & Innovation 24 (2021) 102060

Contents lists available at ScienceDirect

Environmental Technology & Innovation

journal homepage: www.elsevier.com/locate/eti

Ciprofloxacin, ranitidine, and chlorphenamine removal from aqueous solution by adsorption. Mechanistic and regeneration analysis

Cinthia Berenice García-Reyes [a,b], Jacob Josafat Salazar-Rábago [a,*], Manuel Sánchez-Polo [b], Margarita Loredo-Cancino [a], Roberto Leyva-Ramos [c]

[a] Universidad Autónoma de Nuevo León, Facultad de Ciencias Químicas, Av. Universidad S/N, Cd. Universitaria, San Nicolás de los Garza, N.L., 66455, Mexico
[b] Departamento de Química Inorgánica, Facultad de Farmacia, Universidad de Granada, Campus Universitario de Cartuja, Granada, Granada, C.P. 18071, Spain
[c] Centro de Investigación y Estudios de Posgrado, Facultad de Ciencias Químicas, Universidad Autónoma de San Luis Potosí, Av. Dr. M. Nava, San Luis Potosí, S.L.P., 78210, Mexico

ARTICLE INFO

Article history:
Received 6 August 2021
Received in revised form 23 October 2021
Accepted 26 October 2021
Available online 1 November 2021

Keywords:
Adsorption
Pharmaceuticals
Emerging pollutants
Tertiary treatment
Cycles
Reuse

ABSTRACT

Several studies have reported the presence of pharmaceuticals in freshwater bodies all around the world. For this investigation, the removal of the pharmaceuticals ciprofloxacin (CIP) ranitidine (RNT), and chlorphenamine (CPM) using lignocellulose-derived granular activated carbon (GAC) was analyzed, and the physicochemical mechanisms of removal were elucidated. Additionally, the textural and surface properties of the GAC were evaluated, the concentrations of the contaminants were monitored with UV–Vis Spectrophotometry. The results revealed that GAC is a mesoporous material with a surface area of 940 m^2/g and an acidic character with a point of zero charge (pH_{PZC}) around 2. The adsorption isotherms showed a consistent behavior with the Prausnitz–Radke model, reporting adsorption capacities of 668, 521, and 582 μmol/g (221, 173 and 193 mg/g), at an equilibrium concentration of 50 μmol/L, pH 7 and 25 °C for CIP, RNT and CPM, respectively. Moreover, studies at different pH levels, temperature, and reversibility suggested that adsorption obeys physical mechanisms, which led to the proposal of a chemical regeneration process with organic (ethanol and methanol) and inorganic (NaOH and HCl) diluents. Better results were obtained using the inorganic diluents, ranging between 44 and 73% thermodynamic desorption. Additionally, three reuse cycles were successfully performed at the best conditions, with a regeneration efficiency in the range of 68%–98% for each of the pharmaceuticals. The results demonstrate the viability of the use of GAC for the removal of drugs with different characteristics in scenarios that are very close to the real ones.

1. Introduction

Around the world, the presence of pharmaceutical compounds in surface water has been increasingly reported during the past few years (aus der Beek et al., 2016). Widely used pharmaceuticals such ciprofloxacin (CIP), ranitidine (RNT),

* Corresponding author.
E-mail address: jacob.salazarrb@uanl.edu.mx (J.J. Salazar-Rábago).

https://doi.org/10.1016/j.eti.2021.102060

and chlorphenamine (CPM) have been reported in concentrations between 3 and 923 ng/L in distinct water bodies. Its side effects are not detailed known but the concerns on the affectation on the human health and toxicity are latent since similar substance are reported that harmed the development of living organisms and causing an increase in bacterial resistance to antibiotics (de García et al., 2016; Kostich and Länge, 2016; Tenorio-Chávez et al., 2020).

In addition to this, traditional technologies used in Wastewater Treatment Plants (WWTP) have been known to be inefficient to remove pharmaceutical compounds (Yang et al., 2017). There is a need to apply alternative technological solutions to avoid compromising the health and well-being of the next generations, acknowledging the impossibility of a suspension in the use of pharmaceuticals. Previous research projects have faced this difficulty and dealt with it by proposing the application of adsorption processes for the purification of water that was polluted by pharmaceuticals, given the fact that adsorption is a versatile and straightforward alternative that has been widely studied for the removal of emerging pollutants, owing to its effectiveness even at low concentrations.

The adsorption of pharmaceuticals using raw clays, graphene, nanotubes, activated carbon, among others, has been widely reported (Carrales-Alvarado et al., 2020; de Franco et al., 2017; França et al., 2019; Lin et al., 2019; Mondal et al., 2016; Pauletto et al., 2021; Zhuang et al., 2015). Activated carbon is the most commonly applied since it has a large surface area and a plurality of functional groups whose graphene layers have a strong affinity for organic compounds. It can be prepared by diverse processes, and the precursor material can be biomaterials and non-mineral materials, such as lignocellulosic sources. The activation of the carbons can be chemical or physical. The study of commercial materials on new applications can bring some insights on the versatility of those materials.

In this sense, it is necessary to study activated carbon and the adsorption mechanisms, considering its regeneration for further reuse, contributing to minimizing resource consumption, costs, and environmental impact. The adsorption mechanisms can be found by characterizing the adsorbent material and determining the behavior of the adsorption and desorption capacity under different conditions. This is performed in a range of concentrations of interest to the application. Based on their observation and analysis of these results, it is possible to propose the relevant mechanisms involved (Abbas et al., 2018; Carrales-Alvarado et al., 2020).

Several techniques for regenerating activated carbon have been reported, such as ultrasound, electrochemical processes, and the conventional ones: thermal and chemical regeneration (Chen et al., 2017; El Gamal et al., 2018; Mariño Peacok et al., 2021; Mustafa et al., 2021). From the point of view of the minimization of resource consumption, chemical regeneration stands out as an attractive option, considering that it can be performed in situ with a low energetic cost, minimal loss of adsorbent, and without the need for specialized preparation. However, the viability of this process depends on the interactions between the pollutant and the activated carbon. Consequently, it is essential to be aware of both the adsorption capacity of the material and its dominant mechanisms for a specific adsorbate and to be able to find an efficient regeneration process.

This study aims to perform an accurate analysis of the adsorption mechanisms of the selected model pharmaceuticals: CIP, RNT, and CPM, as representatives of drugs of acidic, amphoteric and basic character, respectively, on a granular activated carbon (GAC) from a lignocellulosic source, as well as to propose a regeneration process for the latter, to serve as the basis for a technological process design to solve the pollution problem.

2. Materials and methods

2.1. Adsorbent

The GAC used in this study was purchased from Jalmek (México) and was obtained from phosphoric acid chemical activation of a lignocellulosic source. Before adsorption experiments, GAC was sieved to obtain a particle size ranging between 425 and 850 μm. The main characteristics of GAC are discussed in Section 3.

2.2. Reagents

Sigma-Aldrich provided the high-purity pharmaceuticals that were used in this study. Some of the physicochemical characteristics of the pharmaceuticals selected for the present study are summarized in Table S1. Table S2 shows the speciation diagram of the molecules and the presence and net charge of each species.

A standard 250 μmol/L solution of each of the pharmaceuticals was prepared, and experimental solutions of the pharmaceuticals were obtained using deionized water. The ionic strength of the solutions was previously established at 0.01 M NaOH, and the pH of the test was adjusted using either NaOH or HCl at 1, 0.1, or 0.01 M.

The concentration of each of the pharmaceuticals in solution was determined by UV–Vis Spectroscopy using a Thermo Scientific Genesys 10S equipment. The wavelength was strategically defined to keep the linear relationship between the absorbance and the concentration. The interval used for the calibration line was 5–50 μmol/L. The wavelengths used at pH 7 for each pharmaceutical were 271, 228, and 261 nm for CIP, RNT, and CPM, respectively.

Some of the reagents were obtained from local companies which meet the standards of the American Chemical Society (ACS): hydrochloric acid 37% (HCl), sodium hydroxide (NaOH), sodium bicarbonate ($NaHCO_3$), sodium carbonate (Na_2CO_3), sodium chloride (NaCl) and ethanol 99.5% (EtOH) from the Desarrollo de Especialidades Químicas company, and methanol 99.9% from Tedia.

2.3. Textural and physicochemical characterization

The surface area and the pore-size distribution were obtained by nitrogen physisorption at 77 K using a Micrometrics TriStar II Plus, where the sample was previously degassed in vacuum conditions during 24 h at 95 °C. BET and BJH models were used to obtain the surface area and the pore-size distribution. Morphology was observed with a FEI QuemScan650F scanning electron microscope (SEM). On the other hand, the surface composition was obtained by means of x-ray photoelectron spectroscopy (XPS) with a Kratos Axis Ultra-DLD instrument.

According to Boehm's method, the functional groups were quantitatively obtained by acid–base titrations, based on a methodology reported in the literature (Salazar-Rabago and Leyva-Ramos, 2016). For each neutralizing solution, 0.1 g of GAC in 25 mL were used, and the corresponding titration was performed five days later. The acidic and basic sites were neutralized with 0.1 N HCl and NaOH, respectively. Additionally, the carboxylic and lactonic sites were titrated with Na_2CO_3, the carboxylic sites with $NaHCO_3$, whereas the phenolic sites were obtained by subtraction between the total acidic sites, the carboxylic, and the lactonic. Each titration was performed twice.

As for the surface charge, twenty-three neutralizing solutions with pH ranging between 1 and 12 were prepared by adding between 0 and 16 mL of 0.1 N NaOH and HCl solutions to 100 mL volumetric flasks and filling up to the mark with a 0.1 N NaCl solution. In a 50 mL polypropylene bottle, 0.2 g of the adsorbent and 45 mL of the various neutralizing solutions were added. Next, nitrogen was bubbled for 2 min to prevent the formation of carbonates in the solution. The bottles were capped and stirred by placing the plastic bottles on top of an orbital shaker at 150 rpm for 15 min every day. The rest of the 100 mL solution was stored without the adsorbent and used as a blank solution. After five days, the final pH of all solutions was measured by a pH meter. The potentiometric curves of both solutions were plotted in the same figure (final pH vs. volume of titrating solution). The intersection of both curves corresponded to the point of zero charge (pH_{PZC}) of the adsorbent. The surface charge was evaluated from both potentiometric curves using the procedure and equation described elsewhere (Leyva-Ramos et al., 2011). The surface charge distribution (surface charge vs. pH) was plotted to explain the role of the electrostatic interactions in the adsorption.

2.4. Adsorption equilibrium

The adsorption equilibrium data were obtained in batch adsorbers, adding 50–100 mg of adsorbent in 45 mL of solution with a known initial concentration of the selected pharmaceutical. The initial pH was established after 30 min from the first contact of the adsorbent with 0.01 M HCl or NaOH solutions, and the pH was controlled every 24 h until reaching equilibrium. Constant agitation was performed within an orbital shaker at 150 rpm. Preliminary tests were carried out to find the equilibrium time of each pharmaceutical, and some experimental conditions were performed twice to measure the experimental error. The experimental points of each isotherm were procured using initial concentrations ranging between 40 and 250 μmol/L.

The adsorption equilibrium tests were carried out at 25 °C and pH 5, 7, and 9; and at different temperatures of 25 and 45 °C keeping the pH at 7, since municipal wastewater typically has a pH near 7 (Hernández-Tenorio et al., 2021; Tenorio-Chávez et al., 2020). The temperature was kept constant using a thermostatic bath.

The amount of pharmaceutical adsorbed on solid (q), provided that the volume of the system and the mass remain constant, can be calculated using the following Eq. (1):

$$q = \frac{V}{m}(C_0 - C_e) \tag{1}$$

where q represents the contaminant uptake (μmol/g), V the volume (L), m the mass of the adsorbent (g), C_0 and C_e the initial concentration and the concentration at the equilibrium of the pharmaceutical in the solution (μmol/L), respectively.

The experimental data for the adsorption equilibrium were adjusted to the Freundlich, Langmuir, and Prausnitz–Radke models, whose equations are shown in (2), (3), and (4), respectively. The parameters for these models were obtained by a nonlinear regression using the least-squares method in STATISTICA software.

$$q_e = K_F C_e^{1/n} \tag{2}$$

$$q_e = \frac{q_m K_L C_e}{1 + K_L C_e} \tag{3}$$

$$q_e = \frac{A C_e}{1 + B C_e^{\beta}} \tag{4}$$

where q_e is the adsorption capacity at equilibrium (μmol/g), K_F is the Freundlich constant related to the adsorption capacity ($\mu mol^{1-1/n}L^{1/n}/g$), n is the intensity of adsorption, q_m is a parameter that represents the maximum adsorption capacity (μmol/g), K_L is the Langmuir model constant related to the heat of adsorption (L/μmol) and A (L/μmol), B ($\mu mol^{\beta}/g^{\beta}$) and β are the parameters of the Prausnitz–Radke isotherm.

Furthermore, the global deviation percentage was calculated (%D) with the experimental data and the calculated data to find which isotherm model best represented the adsorption equilibrium. The %D was estimated by Eq. (5):

$$\%D = \frac{1}{N}\sum_{i=1}^{N}\frac{\left|q_{exp\,i} - q_{cal\,i}\right|}{q_{exp\,i}} \times 100\,\% \tag{5}$$

where N is the number of experiments, $q_{exp\ i}$ the adsorption capacity as measured, and $q_{cal\ i}$ the adsorption capacity obtained with the isotherm model, both in μmol/g.

2.5. Desorption equilibrium data

The adsorption–desorption tests were used to study the reversibility of the adsorption. The adsorption of the pharmaceutical was carried out at pH 7 and 25 °C. The solution was decanted, the GAC was washed with 3 mL of deionized water, and the supernatant solution was removed. Afterward, 40 mL of the buffer solution at pH 5 or 7 were added and allowed to reach equilibrium for the same time the adsorption process took place.

For the desorption experiments, the new equilibrium point was calculated from the subsequent relationship:

$$q_d = q_e - \frac{V}{m}(C_e) \tag{6}$$

where q_d represents the pharmaceutical remaining adsorbed on the surface of the adsorbent and q_e the adsorbed quantity during the adsorption phase, both in μmol/g.

It is proposed to calculate the desorption percentage relative to the thermodynamic equilibrium as an indicator of the reversibility of the process. The $q_{d,rev}$ was estimated using a graphical procedure, where the intersection of the operating line and the resulting adsorption isotherm represents the desorption capacity with 100% reversibility. This procedure will make it possible to obtain the desorption thermodynamics percentage (%DT) with the following equation:

$$\%\mathrm{DT} = \frac{1}{N}\sum_{i=1}^{N}\left|\frac{q_e - q_d}{q_e - q_{d,rev}}\right| \times 100\,\% \tag{7}$$

where $q_{d,rev}$ is the expected mass remaining adsorbed assuming that the adsorption was reversible in μmol/g.

2.6. Regeneration and reuse

For regeneration experiments, an initial concentration of the pharmaceutical and a given mass of the adsorbent were selected. The adsorption process was carried out at 25 °C, pH 7, and an initial concentration between 150 and 200 μM. The solution was decanted, the GAC was washed with 3 mL of deionized water, and the supernatant solution was removed. Afterward, 40 mL of each of the diluents selected for chemical regeneration were added for the same time in which the adsorption process took place.

The amount of pharmaceutical remaining adsorbed on the surface of the GAC was calculated using Eq. (6), and the desorption regeneration percentage (%DR) was obtained by the following equation, which is similar to Eq. (7) but equalizing $q_{d,rev} = 0$, in order to compare and choose the scenario that brings the highest regeneration percentage.

$$\%\mathrm{DR} = \frac{1}{N}\sum_{i=1}^{N}\left|\frac{q_e - q_d}{q_e}\right| \times 100\,\% \tag{8}$$

Adsorption–desorption cycles were carried out consecutively under the best conditions to evaluate the reuse of the adsorbent. Regeneration efficiency was calculated with Eq. (9) (%RE) relating the adsorption capacity of the cycle ($q_{e,r}$) to the initial adsorption capacity ($q_{e,v}$) of the GAC with the following equation (Chen et al., 2017; Larasati et al., 2020):

$$\%\mathrm{RE} = \frac{1}{N}\sum_{i=1}^{N}\left|\frac{q_{e,r}}{q_{e,v}}\right| \times 100\,\% \tag{9}$$

3. Results and discussion

3.1. Adsorbent characterization

The characterization of the GAC revealed its acidic character with a point of zero charge (pH_{PZC}) around 2, the surface is negatively charged at pH values above pH_{PZC}. Figure S1-A shows the charge distribution diagram as a function of the pH, indicating a net negative charge of −70, −120, and −150 C/g at pH 5, 7, and 9, respectively.

In addition, the quantification of the active sites by using Boehm's potentiometric method shows the predominance of the phenolic sites (1.0 meq/g), followed by the carboxylic (0.4 meq/g), while it was not possible to quantify the lactonic sites. As for the basic sites, the total was 0.34 meq/g These results confirm with the acidic characteristics of the GAC.

Furthermore, the textural characterization of the material revealed that the GAC is a mesoporous material, presenting a nitrogen adsorption–desorption isotherm of type IV and a hysteresis loop of type H3 according to the IUPAC classification (Figure S1-B). Moreover, the BET method resulted in a surface area of 940 m^2/g, while the BJH method yielded a diameter and average pore volume of 3.8 nm and 0.68 cm^3/g, respectively. The pore size diameter showed that the highest pore volume ranges from 1 to 5 nm (Figure S1-C). Comparing the pore size to the topological polar surface area of the studied

Table 1
Parameters of the isotherm models at equilibrium for the selected pharmaceuticals and conditions. It was obtained by the averages.

Adsorbate	pH	T °C	Freundlich			Langmuir			Prausnitz–Radke				q50 μmol/g
			K_F $\mu mol^{1-1/n}L^{1/n}/g$	n	%D	q_m μmol/g	K_L L/μmol	%D	A L/g	B $L^{\beta}/\mu mol^{\beta}$	β	%D	
CIP	5	25	113.6	3.0	13.8	698	0.042	10.2	51.27	0.188	0.82	11.0	454
	7	25	348.8	6.3	5.8	761	0.170	8.2	104.00	0.165	0.95	8.9	668
	9	25	53.8	2.3	7.4	641	0.018	5.3	19.98	0.121	0.76	4.7	297
	7	45	250.7	3.7	2.3	975	0.081	6.6	312.80	0.956	0.78	2.0	737
RNT	5	25	124.1	3.9	9.1	431	0.090	6.2	35.80	0.096	0.97	5.0	340
	7	25	149.3	3.1	11.7	616	0.111	8.7	66.82	0.104	0.99	8.7	521
	9	25	123.4	2.5	11.8	695	0.089	10.6	74.12	0.164	0.89	10.8	585
	7	45	55.8	1.9	7.7	782	0.029	6.3	24.12	0.040	0.95	6.9	456
CPM	5	25	116.6	3.2	5.7	641	0.041	6.6	24.60	0.055	0.93	7.7	398
	7	25	236.3	4.3	12.2	785	0.077	8.2	49.00	0.095	0.90	9.5	582
	9	25	202.8	3.2	15.3	1048	0.047	10.7	42.00	0.050	0.95	11.0	687
	7	45	119.6	2.5	7.9	1071	0.025	3.2	30.79	0.038	0.96	5.5	587

Table 2
Atomic concentration obtained by XPS, for the GAC before adsorption and with each of the pharmaceuticals adsorbed. Values represented in %.

	GAC	C-CIP	C-CIP-R	C-RNT	C-RNT-R	C-CPM	C-CPM-R
C 1s	85.5	82.1	80.8	82.3	82.6	82.0	82.2
O 1s	13.7	13.2	13.2	13.4	13.7	12.6	13.1
N 1s	0.1	2.7	2.2	3.0	2.6	4.3	3.9
P 2p	0.8	0.2	0.2	0.3	0.2	0.2	0.2
S 2p		0.2		0.5	0.7	0.1	0.3
Cl 2p		0.1	0.2	0.2	0.1	0.4	0.3
Na 1s		0.6	3.0	0.4	0.1	0.4	
F 1s		0.7	0.5				

molecules (which ranges between 0.161 and 1.12 nm^2), it was considered beneficial to have this pore size distribution for the adsorption of the selected pharmaceuticals, thus avoiding possible steric and geometric impediments between the molecules and the pores of the selected adsorbent, which could affect the adsorption and desorption processes.

The morphology observed by the scanning electron microscope is presented in the supplementary material (Figure S1-D and E), which correspond to the typical morphology observed for activated carbon particles from a wood precursor. The XPS analysis on the GAC revealed the predominance of carbon and oxygen. Table 2 presents the quantified atomic percentages, in addition to the aforementioned elements, nitrogen and phosphorus were also identified, the first one associated to the biomass of the precursor material and the latter related to the activating agent used during the synthesis of the material. High resolution analysis in the C1s, O1s and N1s regions is presented in Figure S10, said analysis revealed the presence of hydroxyl, carbonyl and carboxylic groups (Moreno-Castilla et al., 2000), however signals related to nitrogen bonding were not detected, this is attributed to the low concentration of this element on the surface of the material, this being corroborated by the elementary analysis previously mentioned. Similar results have been obtained by diverse authors for diverse GACs (Jansen and van Bekkum, 1995; Moreno-Castilla et al., 2000).

3.2. Adsorption isotherm

In Table 1, estimated parameters for the adsorption isotherms models are shown, along with the overall deviation percentage for the removal of CIP, RNT, and CPM adsorption. It was noted that both the Langmuir and the Prausnitz–Radke (P–R) models successfully describe most of the analyzed cases. However, the mean overall deviation percentage for the P–R model is 7.6%, compared to 7.7% and 9.2% for the Langmuir and Freundlich models, respectively. Therefore, the adsorption isotherms of the P–R model were considered for the rest of this study. In addition, the adsorption capacity at an equilibrium concentration of 50 μM (q50) was considered a reference value for comparing adsorption capacities. Values of q50 are summarized in the last column of Table 1. In the following sections, the adsorption mechanism will be discussed in detail for each compound.

3.3. CIP – GAC adsorption

The effect of pH on the adsorption isotherms of CIP onto GAC is displayed in Fig. 1-A. It is possible to appreciate that the removal of the pharmaceutical is benefited at pH 7. The q50 estimated values show an increase in contaminant uptake by 47% when pH increases from 5 to 7, while it decreases by 35% as pH changes from 5 to 9. These changes are due to the 50% of the molecules present in the negatively charged species at pH 9, which could be repulsively interacting toward the

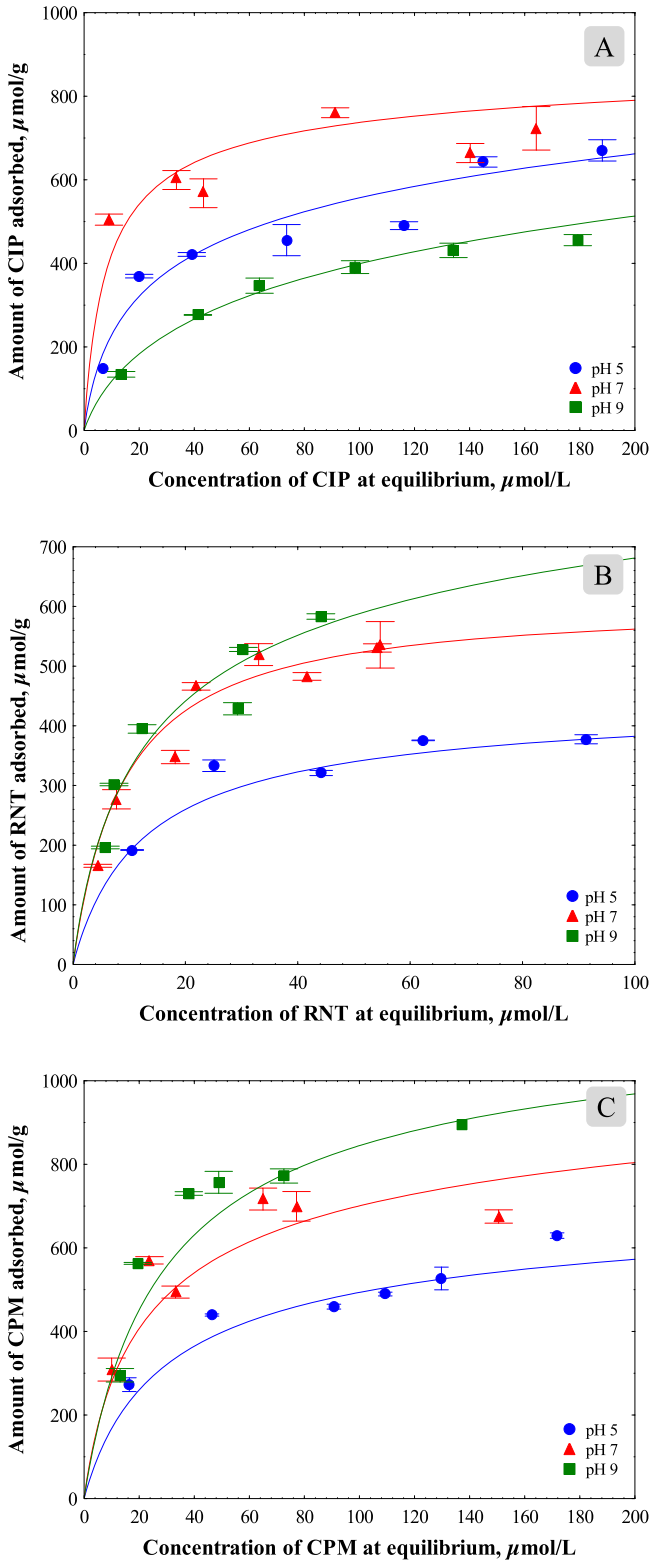

Fig. 1. Adsorption of CIP, RNT and CPM onto GAC at 25 °C. Points correspond to experimental data, error bars are shown. Continuous lines are the P–R model.

carbon surface, abundant in acidic sites. The rest of the molecules are present as zwitterionic species, showing activity in the acidic O^- group and the basic site NH^{2+}, the latter being the one in which attractive interactions toward the surface of the material may occur. Because more than 90% of the molecules have a zwitterionic charge (Table S2), the highest adsorption capacity is found at pH 7, and the aforementioned attractive interactions multiply. Also, 10% of the molecules that are positively charged may show attractive interactions with the surface.

Finally, the adsorption capacity decreases at pH 5 compared to the levels at pH 7, even when there are more positively charged molecules (90% vs. 10%). This decrease suggests that, besides the amino group adsorption, π-π interactions may occur in the zwitterionic species, which could be the reason behind the high adsorption capacity. Other authors have studied the adsorption of CIP onto carbon-based materials, reporting evidence of the hydrophobic interactions (Bizi and El Bachra, 2020; Shang et al., 2016) and the π-π dispersive interactions (Bizi and El Bachra, 2020; Carabineiro et al., 2011) at around pH 7. In contrast, electrostatic interactions were reported at acidic pH values (Bizi and El Bachra, 2020), along with cation–pi interactions (Carabineiro et al., 2011; Sun et al., 2016; Zhang et al., 2017). Previous research reported a decrease in the adsorption capacity as pH increases due to a net repulsion between the negative charge of the molecule and the adsorbent (Zhang et al., 2017). This behavior is consistent with the findings of this study.

Additionally, the effect of temperature on the CIP uptake was analyzed with the q50 data reported in Table 1, where it is possible to observe an increase of around 10% in the amount removed when the temperature is increased from 25 to 45 °C, which may suggest it is an endothermic process (Figure S2).

Reversibility tests were carried out with aqueous solutions at different pH values to elucidate in a better way the adsorbate–adsorbent interactions in the adsorption of CIP onto GAC. The results revealed partial desorption of the pharmaceutical and that the quantity that remains adsorbed is similar at pH 5 and 7 (Figure S3). Additionally, the quantification of the thermodynamic desorption for this pharmaceutical showed a %DT of 53% at pH 7 and 33% at pH 5, which suggests chemical interactions between the CIP and the carbonaceous surface of the adsorbent.

Therefore, it is proposed that the mechanisms present in the adsorption of CIP onto GAC at pH 7 are dispersive interactions that occur due to the presence of zwitterionic species. It is also due to the presence of electrostatic interactions between the positively charged species and the acidic groups of the GAC. Lastly, it is also noted that the incomplete reversibility of the process provides evidence of a chemisorption mechanism that could be due to a cation exchange with the aromatic rings, as previously reported (Carabineiro et al., 2011; Sun et al., 2016; Zhang et al., 2017).

3.4. RNT-GAC adsorption

Fig. 1-B shows the adsorption isotherms of RNT at different pH levels. An increase in the adsorption capacity with respect to pH is registered beyond the concentration at equilibrium of 30 μmol/L. Comparing the q50 values, the amount removed at pH 9 was just 12% higher than that reported at pH 7, while the minimum amount removed was obtained at pH 5 with q50 values that were 53% lower than those obtained at pH 7.

Regarding the molecule, a net positive charge at pH 5 and 7 is observed, and a mainly neutral charge at pH 9, while the surface of the GAC has a negative charge. It is expected that electrostatic interactions occur at pH 5 and 7 due to the difference between the charges and hydrogen bridges between the neutral molecule and the surface of the material at high levels of pH, as a consequence of the activation of the phenolic groups. Although there is no observable significant differences in the predominant species at pH 5 and 7, a remarkable change in the adsorption capacity was noted. This behavior may relate to the increase in the negative charge on the surface of the material.

Other authors have found evidence of the electrostatic interactions between the carbonaceous materials and RNT (Bojić et al., 2017; Das and Goud, 2020; França et al., 2019), along with hydrogen bridges between the neutral molecule and the surface of the material (Abu Al-Rub et al., 2020; França et al., 2019) and even dipole–dipole interactions (Abu Al-Rub et al., 2020).

The adsorption experiments reveal that the remotion capacity decreased as the temperature increased from 25 to 45 °C, indicating an exothermic process (Figure S4).

The thermodynamic reversibility tests for this pharmaceutical showed partial desorption, with a %DT of 75 at pH 7 and of 71% at pH 5, meaning this was the best reversibility value found in this study (Figure S5). The fact that the desorption was partial, though, suggest the existence of chemical interactions, as there is no ability to achieve complete desorption from the thermodynamic perspective.

The mechanisms identified during the RNT adsorption process onto the GAC are electrostatic interactions between the amino group and the surface of the material, along with hydrogen bridges between the neutral molecule and the phenolic group, and chemical interaction to a lower degree.

3.5. CPM- GAC adsorption.

In regards to the adsorption process of chlorphenamine, the effect of pH on the adsorption capacity can be observed in Fig. 1-C. CPM in its solid form is habitually found as an organic maleate salt, which enhances the affinity between this molecule and the carboxylic groups. Therefore, adsorption is expected to occur over this type of site present on the surface of GAC. The highest adsorption capacity can be found at pH 9; a clear tendency between the increase in pH and the adsorption capacity is also observed, where the q50 of pH 5–7 increases by 46% and the one of pH 7–9 increases by 18%.

Table 3
Desorption regeneration percentages were obtained on average for each of the studied conditions.

	0.1 M NaOH	0.1 M HCl	12.4M MeOH	8.5 M EtOH
CIP	57%	8%	8%	24%
RNT	37%	44%	20%	24%
CPM	28%	73%	37%	36%

According to its speciation diagram, the predominant species of CPM has a positive charge at pH 5 and 7 and would present attractive interactions toward the surface of the GAC. However, a notable change is observed in regards to the adsorption capacity. This behavior can be related to the fact that carboxylic groups are activated at a pH value between 3 and 6. At pH 9, the CPM molecule is 40% neutrally charged, yet a high adsorption capacity is observed, which may be due to dispersive interactions since the electronic cloud is more available thanks to the molecule's stability.

Various authors have deduced that, in carbonaceous materials, some of the mechanisms of this pharmaceutical are mainly electrostatic interactions (Ali et al., 2019; El-Shafey et al., 2016; Sharma et al., 2018), hydrogen bridges (Ali et al., 2019; El-Shafey et al., 2016), ionic exchange (El-Shafey et al., 2016), and chemical adsorption (Sharma et al., 2018).

When the temperature increases from 25 to 45 °C, there is no difference in the adsorption behavior (Figure S6). The thermodynamic reversibility tests for this pharmaceutical achieved a %DT of 56 at pH 7 and 61% at pH 5, presenting partial desorption and showing the existence of chemical interactions (Figure S7). Therefore, the following mechanisms are proposed: dispersive interaction between the aromatic rings of the pharmaceutical and the graphene layers of the GAC, electrostatic interactions between the tertiary amine and the acidic groups of the material, and chemisorption.

3.6. Chemical regeneration

Based on the proposal of the mechanisms present during the adsorption of these pharmaceuticals, in which physical mechanisms are mainly involved, the possibility of carrying out a chemical regeneration process of the material that contravenes the attractive forces present arises. Adsorbent reuse is a simple and affordable option for its extensive scale application (Larasati et al., 2020).

The use of various diluents to achieve the regeneration of carbonaceous materials and reuse the material in subsequent cycles has been reported. Cooney et al. (1983) propose methanol as a solvent for organic compounds, whereas Larasati et al. (2020) note the successfulness of regenerating hydrophobic compounds with a mixture of ethanol and NaOH. Moreover, the use of acids for the same purpose has also been reported in the literature (Valentín-Reyes et al., 2019). This current study has decided to work with four different diluents: two inorganic and two organic, 0.1 M HCl, 0.1 M NaOH, 8.5 M EtOH, and 12.4 M MeOH, incorporating the NaOH as a basic diluent that has not been previously reported.

The desorption regeneration percentages (%DR) were obtained using Eq. (8). The results are shown in Table 3. The CIP case is shown as an example (Fig. 2), where the P–R adsorption isotherm model in a continued line for CIP at pH 7 and 25 °C, while the dotted lines represent the operation lines of adsorption and desorption. It is noted that the four diluents follow the projected operation line, considering the case of HCl, MeOH and EtOH where the equilibrium remains so close to the adsorption isotherm, meaning that the desorption does not move beyond the thermodynamic equilibrium. However, in the case of NaOH, the desorption moved past the aforementioned point of equilibrium, making the regeneration process viable.

Regeneration with NaOH shows a significant advance, matching the observed behavior of the adsorption capacity at different pH levels. Finally, faced with the impossibility of total removal of the pharmaceutical from the surface, the presence of chemical interactions on the molecules strengthens.

For RNT and CPM, the figures are shown in the supplementary material (Figure S8 and S9). As presented in Table 3, desorption of RNT shows the inorganic diluents achieving a higher value than the organic diluents, owing to the water solubility of this molecule. Furthermore, the superiority of the HCl regeneration by 5% compared to NaOH makes it the best result, which is consistent with the previously examined pH effect. The minor difference between these two scenarios suggests that the neutral RNT molecule found at high pH values has a low interaction level with the surface of the material, making it possible to achieve a higher regeneration capacity.

As for the CPM, the inorganic diluent HCl is observed to have the best desorption rate, which corroborates earlier findings regarding the pH effect. The significant difference between the other diluents suggests that the change in polarity and surface of the molecule is the primary mechanism for the desorption of this pharmaceutical. Additionally, organic diluents have been reported to be inefficient for water-soluble compounds (Larasati et al., 2020), such behavior is observed in this study.

In brief, the regeneration of the adsorbent material for CIP was achieved in a solution of 0.1 M NaOH, whereas the best regeneration for RNT and CPM was obtained using 0.1 M HCl. This behavior confirms that electrostatic interactions are one of the dominant mechanisms in the adsorption of these pharmaceuticals since the polarity inversion of the surface and material was beneficial for the surface desorption process. As for the chemical interactions of the molecules and the GAC, an XPS study was performed on samples before and after regeneration (Table 2 and Figure S10).

In the case of the samples obtained after CIP adsorption and GAC regeneration tests (C-CIP and C-CIP-R, respectively), the O/C ratio remains constant, however the N1s proportion increased 27 and 22 times respectively (Table 2). Furthermore,

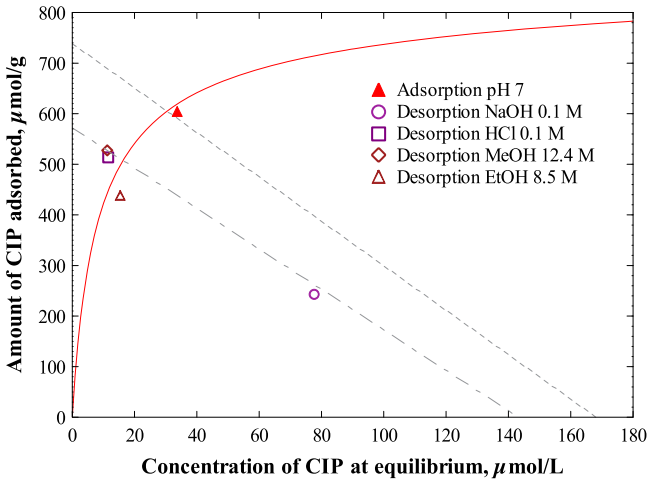

Fig. 2. CIP Desorption tests with various media. Solid line: P–R isotherm model at 25 °C and pH 7. Dashed lines: adsorption and desorption operation lines. Conditions for the adsorption: C_0: 180 micromolar, m_0 0.01 g.

it was possible to quantify C12p and F1s on the surface of both carbons, both heteroatoms present in the molecular structure of the drug (Table S2). This demonstrates, for on part, that the drug is adsorbed and that it remains adsorbed even after the regeneration of the material, suggesting the presence of chemisorption mechanisms. On the other hand, the high resolution analysis shown in Figure S10-A for C1s reveals that the samples containing adsorbed CIP increased their intensity around 286 eV, this can be adjudicated to C–N bonds (Jansen and van Bekkum, 1995; Okpalugo et al., 2005), spectra in the O1s regions show an increase in the carbonyl bonds region (531.2 eV), finally, the analysis on the N1s region reveals a wide curve in the N–C bond region associated to terminal groups such as amines, amides and imides (399.6 eV) (Okpalugo et al., 2005) and C–N–C bonds associated to heterocycles such as pyrroles (400.9 eV) (Jansen and van Bekkum, 1995).

For the GAC samples obtained after RNT adsorption and the regeneration of the material (C-RNT and C-RNT-R, respectively). It can be observed that the carbon and oxygen proportions remain constant when compared to the original material, however, the presence of sulfur and nitrogen stand out, the latter being up to 30 times more that in the pristine GAC, both elements present in RNT's molecular structure The high-resolution analysis on the C1s and O1s presented in Figure S10-A and B show a similar behavior to the one shown by CIP, however the N1s spectra is accentuated around 400 eV (Figure S10-C), this region corresponds the N–C bonds present in amine bonds (Jansen and van Bekkum, 1995; Okpalugo et al., 2005), which can be found on RNT's molecular structure.

Elemental quantification for the C-CPM and C-CPM-R samples, which correspond to the GAC with CPM adsorbed and after the regeneration of the material, respectively. Both samples show that the O/C ratio remained constant, however, several heteroatoms, such as nitrogen and chlorine, were detected, both present in the CPM molecule. In the case of nitrogen, it surpassed 40 times the amount when compared to the starting material while chlorine was not detected at all. The high-resolution spectra presented in Figure S10 reveal, similarly to the other drugs, an intensity increase in the C–N bond region of C1s (Jansen and van Bekkum, 1995), while in the O1s region, the predominant signal corresponds to the R–OH bonds associated with hydroxyl and carboxyl groups (Jansen and van Bekkum, 1995; Moreno-Castilla et al., 2000). On the other hand, the spectra in the N1s region shows its maximum intensity between the binding energies corresponding to N–C and C–N–C bonds, 399.6 and 400.9 eV, respectively, this behavior can be due to the conjunction of both signals since CPM has two nitrogenated groups, one corresponding to a tertiary amine and the other to a pyridinic ring (Okpalugo et al., 2005).

All these results are indicative to the presence of CIP, RNT or CPN on the surface of the carbon even after regeneration of the material, indicating the formation of strong adsorbate–adsorbent interactions.

3.7. Reuse of the material.

Starting from the best regeneration scenarios, evaluating the reuse of the material for each adsorbate–adsorbent pair was made. The reuse would be tested during three adsorption and desorption cycles, which were carried out consecutively in the same way described in Section 3.6, only at the best regeneration conditions.

Results for the three pharmaceuticals can be observed in Fig. 3, each cycle consisting of two bars, where the bar represent the amount of adsorbate present on the material's surface at the end of either the adsorption or the desorption. It is noted that for the three pharmaceuticals, GAC is capable of adsorbing after the regeneration, even if this is incomplete. It is also observed that total desorption of the pharmaceuticals is not obtained for any of the studied cycles.

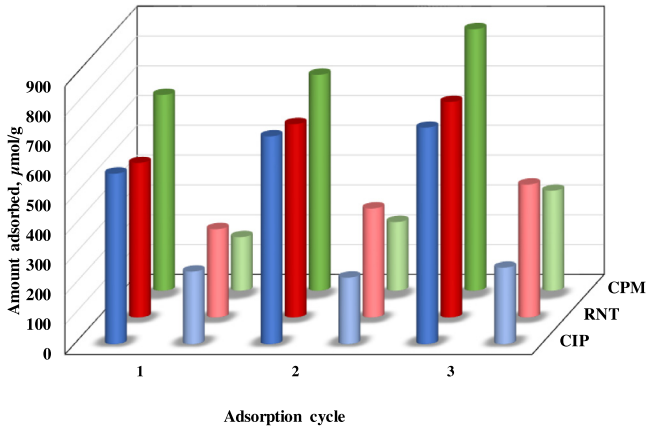

Fig. 3. Adsorption capacity explored in adsorption cycles at pH 7 and desorption in HCl (RNT y CPM) and NaOH (CIP). Bars represent the amount of material on the GAC surface after the adsorption (dark color) and desorption (light color).. (For interpretation of the references to color in this figure legend, the reader is referred to the web version of this article.)

Table 4
Regeneration Efficiency percentages (%RE) were obtained for cycles 2 and 3.

	Cycle		
	1	2	3
CIP	100	79	88
RNT	100	68	69
CPM	100	83	98

Figure S11 shows the equilibrium points from the adsorption and desorption test of every cycle done for CIP and the adsorption isotherm model previously obtained. These results were used to calculate the regeneration efficiency (%RE) with Eq. (9), considering the adsorption capacity of cycle 2 (or 3) with respect to the adsorption capacity of cycle 1, which makes it an indicator of the adsorption capacity of the material after regeneration occurred. Those results are summarized in Table 4.

For the CIP, the adsorption capacity behaved according to the isotherm obtained at pH 7 (Figure S11); the regeneration remained at an average of 63 $\pm$ 6%DR . Values above 80% of regeneration efficiency were obtained, meaning that its adsorption capacity decreased by 20% for the second cycle and only by 12% for the third cycle.

Turning now to the experimental evidence on RNT (Figure S12), it shows a tendency to material saturation, that is to say, a lower regeneration percentage (%DR) in cycles 2 and 3 compared to cycle 1 with an average value of 43 $\pm$ 3% and an increase in the amount of the pharmaceutical remaining on the surface. However, the %RE showed that the adsorption capacity remains close to 70% with respect to the initial adsorption capacity since more RNT can be adsorbed from the surface of the GAC, highlighting that the equilibrium point goes beyond the obtained isotherm. It should be noted that the isotherm calculated at pH 7 has various validated points until an equilibrium concentration of 60 μmol/L.

For the CPM, a similar behavior to RNT is shown, with a regeneration percentage of 68 $\pm$ 5%, obtaining increasing values of %RE, moving from 83% to 98%, from cycle 2 to 3 (Figure S13).

As observed, the retention of molecules post-regeneration was not an obstacle to the adsorption of new molecules. This behavior is possible because the surface of the material is not saturated according to the conditions of the study, which can be corroborated by calculating the surface covered by these, as it has been previously reported in other studies (Carrales-Alvarado et al., 2020), resulting the surface area occupied by the molecules of CPM is 7% and 9% after first and third adsorption cycle, respectively.

The obtained results show that, for this adsorbent, regeneration in 3 cycles is profitable, and the values can be compared to those reported by Cooney et al. (1983), where a range for the loss of adsorption capacity is established between 20 and 25% using organic diluents, or even to the values obtained by Larasati et al. (2020): 78 to 84%RE for small compounds such as phenol, using a mixture of organic and inorganic diluents.

Additionally, the conservation of the adsorbent structure was explored by SEM as a relevant aspect for the reuse of the materials. In the micrography images (Figure S14) is observed the morphology of the GAC after adsorption and after the 3 reuse cycles, which compared with the pristine GAC (Figure S1-D) confirmed the structure is remained unchanged.

4. Conclusions

The adsorption of the pharmaceuticals CIP, RNT, and CPM onto a non-modified GAC was possible. The GAC used for this research work from a lignocellulosic source and chemical activated, is mesoporous material with a high surface

area and acid surface characteristics. The adsorption isotherms were adequately described using the Prausnitz–Radke model with a deviation value 7.6%. The predominant mechanisms for the pharmaceuticals' adsorption were the π-π dispersive interactions, attractive electrostatic interactions, and chemisorption for CIP and CPM, while attractive electrostatic interactions, hydrogen bridges, and chemisorption were present for RNT.

With a majority of physical interactions occurring, a chemical regeneration was carried out with diverse organic and inorganic diluents, finding that the organic solvents were not the most adequate, owing to the high solubility levels of the studied compounds. It is interesting to note that 0.1 M NaOH was the best for CIP, and 0.1 M HCl was the most adequate for RNT and CPM. Reuse cycles of the material were performed at these conditions, achieving a regeneration efficiency above 70% for three cycles, proving the potential of GAC in the removal of pharmaceuticals from water, with the possibility of its regeneration and reuse.

Thus, the workability of the use of the GAC in simulated real case scenarios is demonstrated, giving essential insights and establishing the basis for the application of this type of materials in existing industrial processes for the remediation of drug-contaminated wastewater.

CRediT authorship contribution statement

Cinthia Berenice García-Reyes: Methodology, Formal analysis, Investigation, Writing – original draft, Visualization. **Jacob Josafat Salazar-Rábago:** Conceptualization, Formal analysis, Resources, Writing – reviewing and editing, Supervision, Project administration. **Manuel Sánchez-Polo:** Writing – reviewing and editing, Supervision. **Margarita Loredo-Cancino:** Validation, Writing – reviewing and editing, Supervision. **Roberto Leyva-Ramos:** Supervision.

Declaration of competing interest

The authors declare that they have no known competing financial interests or personal relationships that could have appeared to influence the work reported in this paper.

Acknowledgment

This work was supported by Consejo Nacional de Ciencia y Tecnología, for the schoolarship CVU49215.

Appendix A. Supplementary data

Supplementary material related to this article can be found online at https://doi.org/10.1016/j.eti.2021.102060.

References

Abbas, Z., Ali, S., Rizwan, M., Zaheer, I.E., Malik, A., Riaz, M.A., Shahid, M.R., Rehman, M.Z. ur, Al-Wabel, M.I., 2018. A critical review of mechanisms involved in the adsorption of organic and inorganic contaminants through biochar. Arab. J. Geosci. 11, 448. http://dx.doi.org/10.1007/s12517-018-3790-1.

Abu Al-Rub, F.A., Fares, M.M., Mohammad, A.R., 2020. Use of nanohybrid nanomaterials in water treatment: highly efficient removal of ranitidine. RSC Adv. 10, 37050–37063. http://dx.doi.org/10.1039/D0RA05530A.

Ali, S.N.F., El-Shafey, E.I., Al-Busafi, S., Al-Lawati, H.A.J., 2019. Adsorption of chlorpheniramine and ibuprofen on surface functionalized activated carbons from deionized water and spiked hospital wastewater. J. Environ. Chem. Eng. 7, 102860. http://dx.doi.org/10.1016/j.jece.2018.102860.

aus der Beek, T., Weber, F.-A.A., Bergmann, A., Hickmann, S., Ebert, I., Hein, A., Küster, A., 2016. Pharmaceuticals in the environment-global occurrences and perspectives. Environ. Toxicol. Chem. 35, 823–835. http://dx.doi.org/10.1002/etc.3339.

Bizi, M., El Bachra, F.E., 2020. Evaluation of the ciprofloxacin adsorption capacity of common industrial minerals and application to tap water treatment. Powder Technol. 362, 323–333. http://dx.doi.org/10.1016/j.powtec.2019.11.047.

Bojić, D., Momčilović, M., Milenković, D., Mitrović, J., Banković, P., Velinov, N., Nikolić, G., 2017. Characterization of a low cost Lagenaria vulgaris based carbon for ranitidine removal from aqueous solutions. Arab. J. Chem. 10, 956–964. http://dx.doi.org/10.1016/j.arabjc.2014.12.018.

Carabineiro, S.A.C., Thavorn-Amornsri, T., Pereira, M.F.R., Figueiredo, J.L., 2011. Adsorption of ciprofloxacin on surface-modified carbon materials. Water Res. 45, 4583–4591. http://dx.doi.org/10.1016/j.watres.2011.06.008.

Carrales-Alvarado, D.H., Rodríguez-Ramos, I., Leyva-Ramos, R., Mendoza-Mendoza, E., Villela-Martínez, D.E., 2020. Effect of surface area and physical–chemical properties of graphite and graphene-based materials on their adsorption capacity towards metronidazole and trimethoprim antibiotics in aqueous solution. Chem. Eng. J. 402, 126155. http://dx.doi.org/10.1016/j.cej.2020.126155.

Chen, Q., Liu, H., Yang, Z., Tan, D., 2017. Regeneration performance of spent granular activated carbon for tertiary treatment of dyeing wastewater by Fenton reagent and hydrogen peroxide. J. Mater. Cycles Waste Manag. 19, 256–264. http://dx.doi.org/10.1007/s10163-015-0410-y.

Cooney, D.O., Nagerl, A., Hines, A.L., 1983. Solvent regeneration of activated carbon. Water Res. 17, 403–410. http://dx.doi.org/10.1016/0043-1354(83)90136-7.

Das, S., Goud, V.V., 2020. Characterization of a low-cost adsorbent derived from agro-waste for ranitidine removal. Mater. Sci. Energy Technol. 3, 879–888. http://dx.doi.org/10.1016/j.mset.2020.10.009.

El Gamal, M., Mousa, H.A., El-Naas, M.H., Zacharia, R., Judd, S., 2018. Bio-regeneration of activated carbon: A comprehensive review. Sep. Purif. Technol. http://dx.doi.org/10.1016/j.seppur.2018.01.015.

El-Shafey, E.I., Ali, S.N.F., Al-Busafi, S., Al-Lawati, H.A.J., 2016. Preparation and characterization of surface functionalized activated carbons from date palm leaflets and application for methylene blue removal. J. Environ. Chem. Eng. 4, 2713–2724. http://dx.doi.org/10.1016/j.jece.2016.05.015.

França, D.B., Torres, S.M., Filho, E.C.C.S, Fonseca, M.G., Jaber, M., 2019. Understanding the interactions between ranitidine and magadiite: Influence of the interlayer cation. Chemosphere 222, 980–990. http://dx.doi.org/10.1016/j.chemosphere.2019.01.154.

de Franco, M.A.E., de Carvalho, C.B., Bonetto, M.M., Soares, R. de P., Féris, L.A., 2017. Removal of amoxicillin from water by adsorption onto activated carbon in batch process and fixed bed column: Kinetics, isotherms, experimental design and breakthrough curves modelling. J. Clean. Prod. 161, 947–956. http://dx.doi.org/10.1016/j.jclepro.2017.05.197.

de García, S.O., García-Encina, P.A., Irusta-Mata, R., 2016. Dose–response behavior of the bacterium vibrio fischeri exposed to pharmaceuticals and personal care products. Ecotoxicology 25, 141–162. http://dx.doi.org/10.1007/s10646-015-1576-8.

Hernández-Tenorio, R., Guzmán-Mar, J.L., Hinojosa-Reyes, L., Ramos-Delgado, N., Hernández-Ramírez, A., 2021. Determination of pharmaceuticals discharged in wastewater from a public hospital using lc-ms/ms technique. J. Mex. Chem. Soc. 65, 94–108. http://dx.doi.org/10.29356/jmcs.v65i1.1439.

Jansen, R.J.J., van Bekkum, H., 1995. XPS Of nitrogen-containing functional groups on activated carbon. Carbon N. Y. 33, 1021–1027. http://dx.doi.org/10.1016/0008-6223(95)00030-H.

Kostich, M., Länge, R., 2016. Ecotoxicology, environmental risk assessment and potential impact on human healthy. Issues Environ. Sci. Technol. http://dx.doi.org/10.1039/9781782622345-00180.

Larasati, A., Fowler, G.D., Graham, N.J.D., 2020. Chemical regeneration of granular activated carbon: preliminary evaluation of alternative regenerant solutions. Environ. Sci. Water Res. Technol. 6, 2043–2056. http://dx.doi.org/10.1039/D0EW00328J.

Leyva-Ramos, R., Berber-Mendoza, M.S., Salazar-Rabago, J., Guerrero-Coronado, R.M., Mendoza-Barron, J., 2011. Adsorption of lead(II) from aqueous solution onto several types of activated carbon fibers. Adsorption 17, 515–526. http://dx.doi.org/10.1007/s10450-010-9313-3.

Lin, C.H., Li, C.M., Chen, C.H., Chen, W.H., 2019. Removal of chlorpheniramine and variations of nitrosamine formation potentials in municipal wastewaters by adsorption onto the GO-Fe3O4. Environ. Sci. Pollut. Res. 26, 20701–20711. http://dx.doi.org/10.1007/s11356-019-05278-9.

Mariño Peacok, T., Crespo Sariol, H., Sánchez Roca, Á., Puente Torres, J., Gryglewicz, G., Yperman, J., Carleer, R., Vandamme, D., Reggers, G., Vanreppelen, K., Cuyvers, G., Vercruysse, W., Salomón García, L., 2021. Efficiency evaluation of thermally and chemically regenerated activated carbons used in a water cleaning system by acoustic emission analysis. J. Porous Mater. 28, 451–469. http://dx.doi.org/10.1007/s10934-020-01005-9.

Mondal, S., Aikat, K., Halder, G., 2016. Ranitidine hydrochloride sorption onto superheated steam activated biochar derived from mung bean husk in fixed bed column. J. Environ. Chem. Eng. 4, 488–497. http://dx.doi.org/10.1016/j.jece.2015.12.005.

Moreno-Castilla, C., López-Ramón, M., Carrasco-Mariıń, F., 2000. Changes in surface chemistry of activated carbons by wet oxidation. Carbon N. Y. 38, 1995–2001. http://dx.doi.org/10.1016/S0008-6223(00)00048-8.

Mustafa, M., Kozyatnyk, I., Gallampois, C., Oesterle, P., Östman, M., Tysklind, M., 2021. Regeneration of saturated activated carbon by electro-peroxone and ozonation: Fate of micropollutants and their transformation products. Sci. Total Environ. 776, 145723. http://dx.doi.org/10.1016/j.scitotenv.2021.145723.

Okpalugo, T.I.T., Papakonstantinou, P., Murphy, H., McLaughlin, J., Brown, N.M.D., 2005. High resolution XPS characterization of chemical functionalised MWCNTs and SWCNTs. Carbon N. Y. 43, 153–161. http://dx.doi.org/10.1016/j.carbon.2004.08.033.

Pauletto, P.S., Lütke, S.F., Dotto, G.L., Salau, N.P.G., 2021. Adsorption mechanisms of single and simultaneous removal of pharmaceutical compounds onto activated carbon: Isotherm and thermodynamic modeling. J. Mol. Liq. 336, 116203. http://dx.doi.org/10.1016/j.molliq.2021.116203.

Salazar-Rabago, J.J., Leyva-Ramos, R., 2016. Novel biosorbent with high adsorption capacity prepared by chemical modification of white pine (Pinus durangensis) sawdust, Adsorption of Pb(II) from aqueous solutions. J. Environ. Manage. 169, 303–312. http://dx.doi.org/10.1016/j.jenvman.2015.12.040.

Shang, J.G., Kong, X.R., He, L.L., Li, W.H., Liao, Q.J.H., 2016. Low-cost biochar derived from herbal residue: characterization and application for ciprofloxacin adsorption. Int. J. Environ. Sci. Technol. 13, 2449–2458. http://dx.doi.org/10.1007/s13762-016-1075-3.

Sharma, A., Thakur, K.K., Mehta, P., Pathania, D., 2018. Efficient adsorption of chlorpheniramine and hexavalent chromium (Cr(VI)) from water system using agronomic waste material. Sustain. Chem. Pharm. 9, 1–11. http://dx.doi.org/10.1016/j.scp.2018.04.002.

Sun, Y., Li, H., Li, G., Gao, B., Yue, Q., Li, X., 2016. Characterization and ciprofloxacin adsorption properties of activated carbons prepared from biomass wastes by H3PO4 activation. Bioresour. Technol. 217, 239–244. http://dx.doi.org/10.1016/j.biortech.2016.03.047.

Tenorio-Chávez, P., Cerro-López, M., Castro-Pastrana, L.I., Ramírez-Rodrigues, M.M., Orozco-Hernández, J.M., Gómez-Oliván, L.M., 2020. Effects of effluent from a hospital in Mexico on the embryonic development of zebrafish, Danio rerio. Sci. Total Environ. 727, 138716. http://dx.doi.org/10.1016/j.scitotenv.2020.138716.

Valentín-Reyes, J., García-Reyes, R.B., García-González, A., Soto-Regalado, E., Cerino-Córdova, F., 2019. Adsorption mechanisms of hexavalent chromium from aqueous solutions on modified activated carbons. J. Environ. Manage. 236, 815–822. http://dx.doi.org/10.1016/j.jenvman.2019.02.014.

Yang, Y., Ok, Y.S., Kim, K.H., Kwon, E.E., Tsang, Y.F., 2017. Occurrences and removal of pharmaceuticals and personal care products (PPCPs) in drinking water and water/sewage treatment plants: A review. Sci. Total Environ. http://dx.doi.org/10.1016/j.scitotenv.2017.04.102.

Zhang, B., Han, X., Gu, P., Fang, S., Bai, J., 2017. Response surface methodology approach for optimization of ciprofloxacin adsorption using activated carbon derived from the residue of desilicated rice husk. J. Mol. Liq. 238, 316–325. http://dx.doi.org/10.1016/j.molliq.2017.04.022.

Zhuang, Y., Yu, F., Ma, J., Chen, J., 2015. Adsorption of ciprofloxacin onto graphene-soy protein biocomposites. New J. Chem. 39, 3333–3336. http://dx.doi.org/10.1039/c5nj00019j.